# Mannich base PIP-199 is a chemically unstable pan-assay interference compound

Xinyi Wu, Haritha Krishna Sudhakar, Lisa J. Alcock,* Yu Heng Lau*

School of Chemistry, The University of Sydney, Eastern Ave, Camperdown, NSW 2006, Australia

**ABSTRACT:** PIP-199 is the only reported small molecule inhibitor of FANCM-RMI, a key protein-protein interaction that governs genome instability in the genetic disorders Fanconi Anemia and Bloom's Syndrome. PIP-199 and close analogues that share the same indole-derived Mannich base core scaffold have been used as commercially available tool compounds for studying a wide range of therapeutically relevant biological pathways and targets, including the Alternative Lengthening of Telomeres (ALT), G-quadruplexes, pro-apoptotic proteins, and quorum sensing. Herein, we report the first published synthesis of PIP-199 and related analogues, demonstrating that the parent compound immediately decomposes in common aqueous buffers and some organic solvents. We characterize the breakdown products and show that PIP-199 and its more hydrolytically stable analogues show no observable activity in binding and competitive biophysical assays for FANCM-RMI. We conclude that PIP-199 is not an effective tool compound for biological studies, and that apparent activity in cellular studies likely arises from non-specific toxicity of mixed breakdown products. More generally, apparent inhibitors that share this indole-derived Mannich scaffold potentially represent a new family of pan-assay interference compounds (PAINS) that should be thoroughly assessed for aqueous stability prior to use in biological studies.

## INTRODUCTION

Chemical inhibitors are vital tools for interrogating biological pathways that underpin disease. Inhibitory tool compounds can also serve as structural leads for downstream drug development efforts. A common limitation of screening-derived tool compounds reported in academic literature is the depth of available chemical and biophysical validation data.[1] There are many instances of pan-assay interference compounds (PAINS) and invalid metabolic panaceas (IMPs) that are prevalent in the medicinal chemistry and biology literature, where their apparent activity has later been discovered to arise from off-target behavior.[2-7] Continued use of these unsuitable tool compounds in subsequent studies represents an immense waste of valuable scientific resources, generating invalid conclusions that can convolute scientific progress.

While investigating the Alternative Lengthening of Telomeres (ALT) pathway as a potential target for developing new cancer therapeutics, we encountered the compound PIP-199 (**1**) as the only reported small molecule inhibitor of the FANCM-RMI protein-protein interaction.[8] FANCM-RMI was originally studied as a mediator of genome instability linking the genetic disorders Fanconi Anemia and Bloom's Syndrome,[9] mediating homologous DNA repair mechanisms that are also essential for the survival of ALT-positive cancer cells.[10-15] PIP-199 was identified in an academic high-throughput screening campaign against FANCM-RMI and reported to bind the RMI1/RMI2 core complex in various orthogonal biophysical assays.[8]

Since its report, commercially supplied PIP-199 (Figure 1) has been used in the literature as a tool compound for interrogating ALT in human cancer osteosarcoma models,[10] in vertebrate ALT models,[16] and to interrogate the prevalence and role of G-quadruplexes in the ALT mechanism.[11] Concerningly, PIP-199 and analogues (**2-6**) were also identified under different compound names in an earlier screening campaign against quorum sensing in bacteria, showing potent non-competitive inhibition of *N*-acyl-homoserine lactone synthase in *Burkholderia mallei*.[17] Furthermore, close analogues of PIP-199 have been identified as activators of the pro-apoptotic protein Bax (**4-6**),[18] potential anti-schistosomal compounds in *Schistosoma mansoni* (**7**),[19-20] and potential inhibitors of membrane-bound monoamine transporters (**8**),[21] along with appearances in numerous other publications and patents.[22-28]

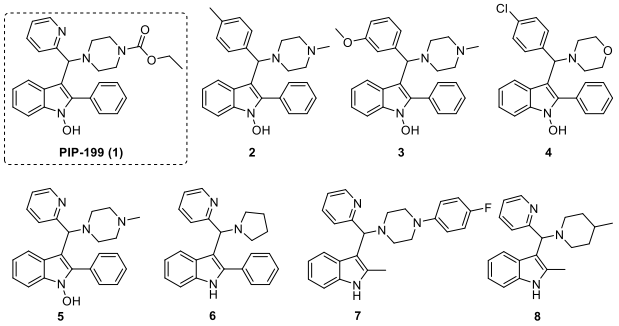


**Figure 1.** Structure of PIP-199 (**1**) and selected analogues reported in diverse medicinal chemistry literature (**2-8**). [10-11, 16-21]

In this light, we report the first published literature synthesis of PIP-199 and unequivocally show that it is an unstable molecule when dissolved in common aqueous buffers as well as some organic solvents, raising significant

questions about the interpretation of data obtained using this compound and its close analogues in biological studies.

## RESULTS AND DISCUSSION

**Chemistry.** With no published synthetic route for PIP-199, we employed a one-pot Mannich route to access the trisubstituted compound (Scheme 1). Reaction of 2-picolinaldehyde **9** with piperazine-1-carboxylic acid ethyl ester **10** in the presence of acetic acid gave the Schiff base intermediate **11**, which upon addition of 2-phenyl-*N*-hydroxyindole **12** gave the Mannich base PIP-199 in reasonable yield.

**Scheme 1.** One-pot synthesis of PIP-199.

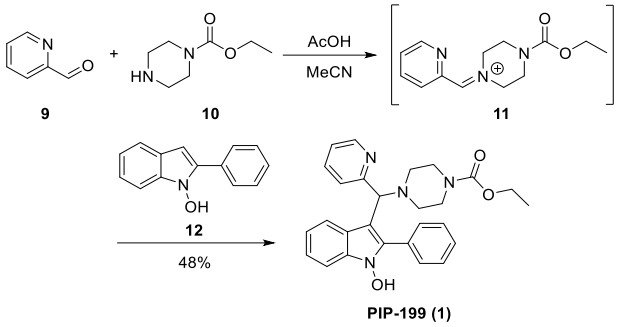


During routine purification and characterization of the product, we discovered that PIP-199 rapidly decomposed during silica column chromatography and in common deuterated NMR solvents, including $CDCl_3$, $CD_3OD$, and wet $CD_3CN$ (Figure 2, SI Figure S1-3). Using a precipitation protocol instead of chromatography, we were able to obtain pure PIP-199 and record its NMR spectrum in DMSO-$d_6$. In addition, PIP-199 was found to remain stable when dissolved in ethyl acetate.

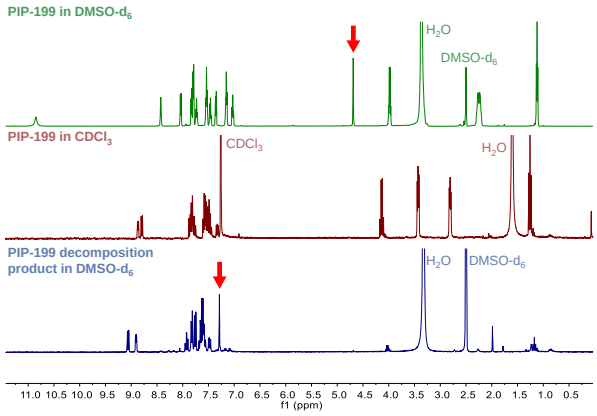


**Figure 2.** $^1$H NMR spectra of PIP-199 in DMSO-$d_6$ (top), $CDCl_3$ (middle), and purified PIP-199 decomposition product in DMSO-$d_6$ (bottom). PIP-199 fully decomposed in $CDCl_3$, based on re-analysis of purified decomposition products by NMR in DMSO-$d_6$ showing complete loss of aliphatic peaks corresponding to the piperazine group (bottom). Diagnostic changes in the central C-H peak are indicated with red arrows. Similar spectra were obtained in $CD_3OD$ and wet $CD_3CN$ (SI Figure S2-3).

Intrigued by the decomposition of PIP-199, we designed a range of structural analogues with the aim of increasing chemical stability. Given the potentially reactive nature of the *N*-hydroxyindole moiety, we synthesized several non-hydroxylated indole analogues **13a-d**, along with a 2-naphthol isosteric analogue **14**. The same Mannich conditions were found to be effective in all cases (Scheme 2).

**Scheme 2.** Synthesis of PIP-199 analogues.

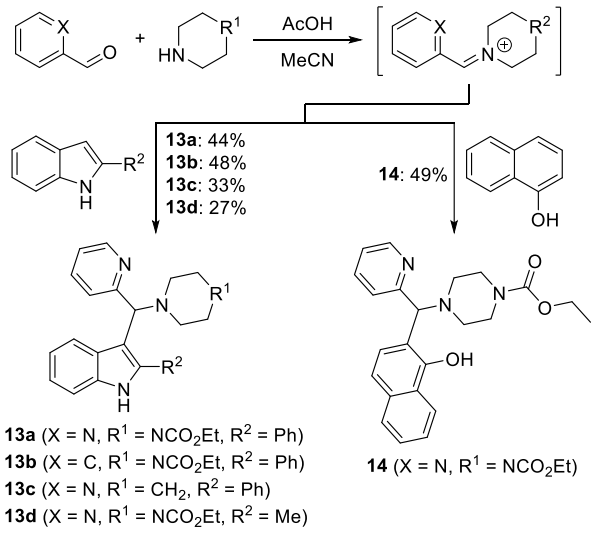


Non-hydroxylated PIP-199 analogue **13a** was compatible with silica column chromatography and displayed improved stability in various deuterated NMR solvents (SI Figure S4). From analogue **13a**, substituting the pyridine for a phenyl ring (**13b**) or the piperazine unit for a piperidine (**13c**) was also well tolerated. However, changing the 2-phenylindole to 2-methylindole (**13d**) seemed to lead to partial degradation during chromatography, while attempts to synthesize the analogue with no substituent at the indole 2-position ($R^2$ = H) were unsuccessful, indicating the importance of the 2-phenyl substituent for stability. Meanwhile, the 2-naphthol analogue **14** was also found to be stable, further implicating the *N*-hydroxyindole as the driver of PIP-199 instability.

**Stability of PIP-199 in aqueous buffer.** We subsequently interrogated whether PIP-199 was unstable under aqueous conditions, focusing on buffers that were reported in literature assays conducted on the compound.[8, 10] In addition to testing various buffer salts and concentrations, we paid close attention to the pH dependence of any observed instability, given that decomposition was initially observed in mildly acidic or protic organic solvents. Due to the limited solubility of PIP-199 in aqueous buffers, as well as overlapping NMR signals arising from buffer salts, the compound was first dissolved in DMSO, diluted into the appropriate buffer. After 1.5 h, the solution was extracted with ethyl acetate, and the extracted material was dried and re-dissolved in DMSO-$d_6$ for $^1$H NMR analysis.

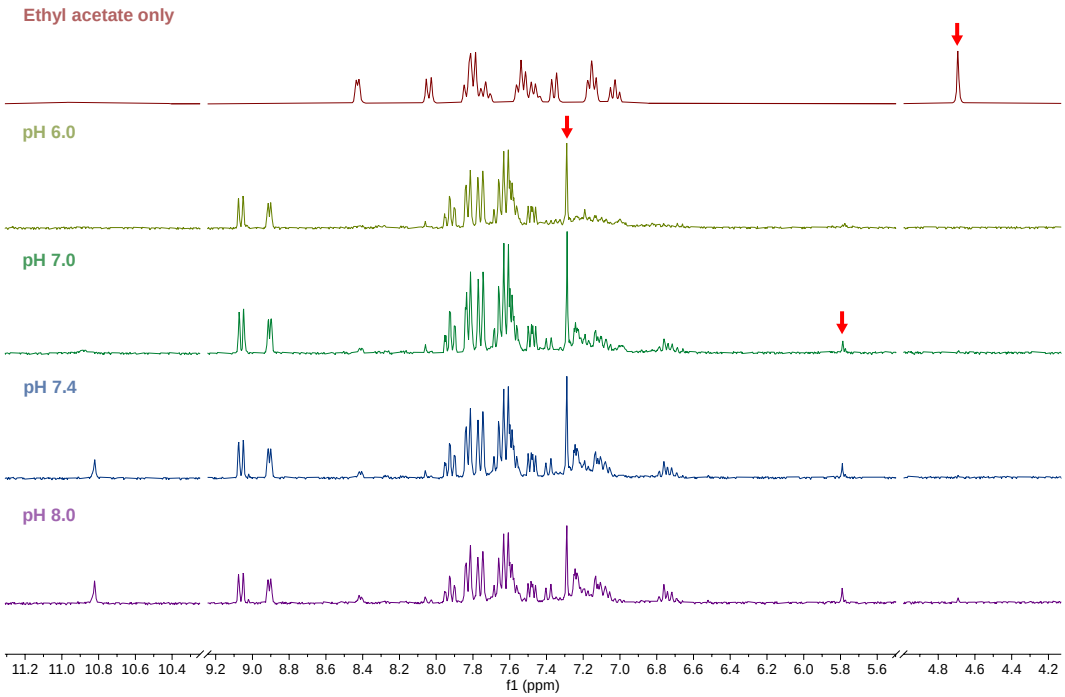


**Figure 3.** $^1$H NMR spectra of PIP-199 after dissolution in phosphate buffers (pH 6-8), extraction with ethyl acetate, and re-dissolution in DMSO-$d_6$. Diagnostic peak changes corresponding to the central C-H signal are indicated with red arrows. Relative integration values for the diagnostic peaks are depicted in Figure 5.

Initial buffer stability tests were conducted in 50 mM potassium phosphate buffer to avoid the appearance of buffer peaks in $^1$H NMR, with almost complete decomposition of PIP-199 observed across the entire buffer pH range (Figure 3). Decomposition was characterized by disappearance of the distinctive PIP-199 singlet at δ 4.7 ppm (central tertiary carbon C-H) and the appearance of a sharp singlet at δ 7.3 ppm, along with a downfield shift of two aromatic apparent doublet peaks (δ 8.9 and 9.1 ppm). Matching integration of these peaks suggested the formation of a single major decomposition product, while another noticeable but weaker pH-dependent singlet at δ 5.8 ppm was likely originating as a secondary byproduct.

To shed light on the identity of the possible breakdown products, reverse phase LCMS analysis of PIP-199 was conducted using a standard $H_2O$/MeCN gradient with 0.1% formic acid, where solid powder was directly dissolved in a 50:50 mix of $H_2O$/MeCN and analysed. Under these acidic aqueous conditions, complete decomposition of PIP-199 was observed (Figure 4 and SI Figure S5). Consistent with the NMR data, a single major species was observed ($t_R$ = 11.4 min) with an *m/z* ratio of 299.15 likely corresponding to the elimination of the piperazine and formation of indolic nitrone **15** (Scheme 3). The combination of the vinylic central proton and the electron-withdrawing nature of the nitrone account for the observed NMR singlet at δ 7.3 ppm and the aromatic peaks at δ 8.9 and 9.1 ppm respectively. While nitrone **15** could not be fully purified by chromatography, NMR of the partially purified material confirmed the loss of piperazine group, matching the postulated structure (Figure 2, Scheme 3, and SI Figure S60).

LCMS analysis also revealed a minor product with an *m/z* ratio of 317.15 ($t_R$ = 8.2 min), potentially corresponding to a secondary alcohol **16** arising from addition of water, accounting for the minor NMR singlet observed at δ 5.8 ppm. Another minor product with an *m/z* ratio of 301.15 ($t_R$ = 9.0 min) was observed, possibly corresponding to a reduction of **15** or loss of the N-hydroxy group from **16**, although it is less mechanistically clear how either process could occur. Finally, another minor peak was observed ($t_R$ = 9.5 min), which might be an isomer of the nitrone due to the appearance of the same parent *m/z* ratio of 299.15.

**Scheme 3.** Postulated mechanism for PIP-199 decomposition under aqueous conditions.[29]

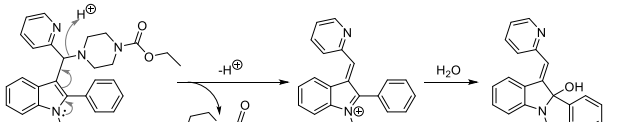


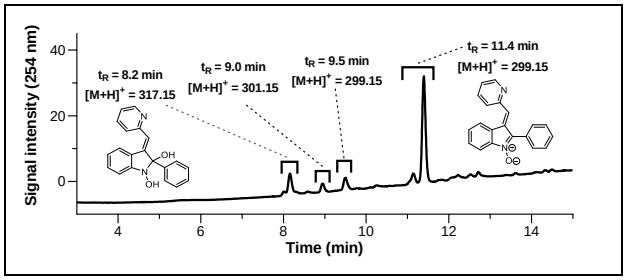


**Figure 4.** LCMS analysis of PIP-199 decomposition in $H_2O$/MeCN with 0.1% formic acid, including possible structures of breakdown products. Mass spectra are shown in SI Figure S5.

In an attempt to track the kinetics of decomposition, we characterized PIP-199 and partially purified nitrone **15** by UV-Vis spectroscopy. In DMSO, the $\lambda_{max}$ values were 253 and 299 nm for PIP-199 and 351 and 431 nm for nitrone **15** (SI Figure S7). However, upon dilution of PIP-199 into phosphate buffer at pH 7 or 8, complete conversion to a spectrum matching that of nitrone **15** had occurred by the time the first spectroscopic measurement was taken (SI Figure S8). This result indicates that PIP-199 almost fully decomposes within seconds in phosphate buffer.

To further investigate the effect of pH and buffer salts on PIP-199 decomposition, as well as to reproduce the conditions used in previous biological studies,[8, 10] we extended stability testing to HEPES, Tris, and ammonia (Figure 5). While the majority of PIP-199 decomposed in all buffer conditions tested, greater stability was observed in 50 mM Tris pH 8.8 buffer alone. As this stabilization was not observed in 10 mM Tris, this result implies that Tris buffer molecule itself may act to stabilize PIP-199 in solution. Nitrone **15** was the dominant species in solution in all other cases, except for 50 mM ammonia at pH 8.8 where the postulated secondary alcohol **16** was the major product. One possible explanation is that ammonia may promote the hydration of the nitrone potentially through nucleophilic attack followed by substitution with water.

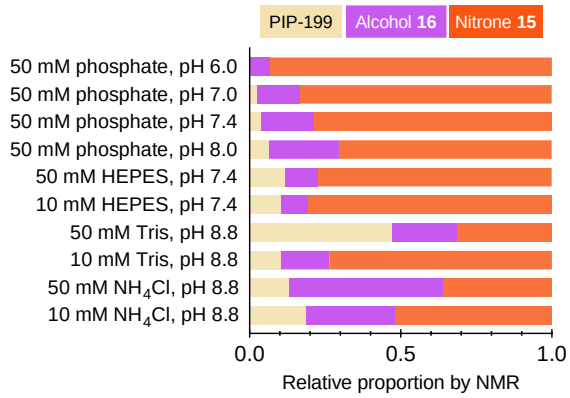


**Figure 5.** Relative proportion of PIP-199 and its breakdown products alcohol **16** and nitrone **15** after exposure to various common buffer conditions for 1.5 h, quantified by comparing NMR integration values at δ 4.7, 5.8 and 7.3 ppm respectively. Phosphate buffer data corresponds to spectra in Figure 3 and full NMR for all conditions are in SI Figures S24-26, 28-35.

**Stability of non-hydroxylated analogue 13a in aqueous buffer.** Given the relative stability of the closest PIP-199 analogue **13a** in organic solvents, its stability in aqueous buffer was also investigated. LCMS analysis under acidic conditions showed the formation of a major byproduct at $t_R$ = 7.3 min with an *m/z* ratio of 301.15 (Figure 6 and SI Figure S6), along with a minor amount of intact **13a** ($t_R$ = 8.7 min, *m/z* = 441.30). By NMR, exposure to phosphate buffer did not change the $^1$H spectrum of **13a** at pH 7-8, while 50% decomposition was observed after exposure at pH 6, including clear doublets emerging at δ 6.8 and 5.8 ppm and reduction in the characteristic tertiary proton singlet at δ 4.9 ppm, along with a number of other new aromatic peaks (Figure 7 and SI Figure S36-39).

Taken together, the NMR and LCMS data indicate that **13a** has improved aqueous stability relative to PIP-199 and is only unstable under acidic conditions, where the major breakdown product is secondary alcohol **17** that forms due to substitution of the piperazine with a hydroxy group. While an *m/z* signal of 283.20 was also observed in the mass spectra of both species, suggestive of the vinylic indolium species analogous to nitrone **15**, we suspect this product only forms during ionization for mass spectrometry, as no corresponding $^1$H NMR peak was observed.

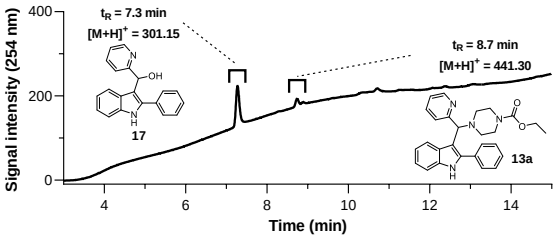


**Figure 6.** LCMS analysis of **13a** decomposition in $H_2O$/MeCN with 0.1% formic acid, including structure of secondary alcohol **17** as a possible breakdown product. Mass spectra are shown in SI Figure S6.

**Binding and competition assays.** To determine the impact of PIP-199 instability on biophysical assays for quantifying disruption of the FANCM-RMI interaction, we first attempted a competitive fluorescence polarization (FP) assay based on the original published reports.[8] While the literature reports used a FITC-labelled 37-mer peptide tracer containing 34 residues from the MM2 domain of FANCM that binds RMI1/RMI2, we made a minor modification by using an *N*-terminally TAMRA-labelled 20-mer peptide centered around the known 12 binding residues based on the original reported crystal structure and associated mutagenesis data.[30] This shorter tracer was more synthetically tractable and showed similar potent binding to RMI1/RMI2 in a direct FP assay (SI Figure S9). However, we noted that at the reported high concentration DMSO of 7.5%v/v, the assay response was negatively influenced with higher IC50 values (SI Figure S10). For this reason, we chose a lower value of 3.75%v/v DMSO to perform our assays to achieve more consistent results.

PIP-199 was unable to displace the fluorescent tracer in our competitive FP assay when using either buffer conditions similar to those published (10 mM Tris, 40 mM NaCl, 2 mM 2-mercaptoethanol, pH 8.8, SI Figure S11) or our standard buffer conditions (50 mM Tris, 200 mM NaCl, 2 mM 2-mercaptoethanol, pH 8, SI Figure S12). Furthermore, none of the more stable analogues (**13a-d**, **14**) showed any change in anisotropy signal in the same competitive FP assay (SI Figure S12). Notably, we observed precipitation for PIP-199 at concentrations above 250 μM, thus we were unable to reproduce the most concentrated data points reported in the literature.[8]

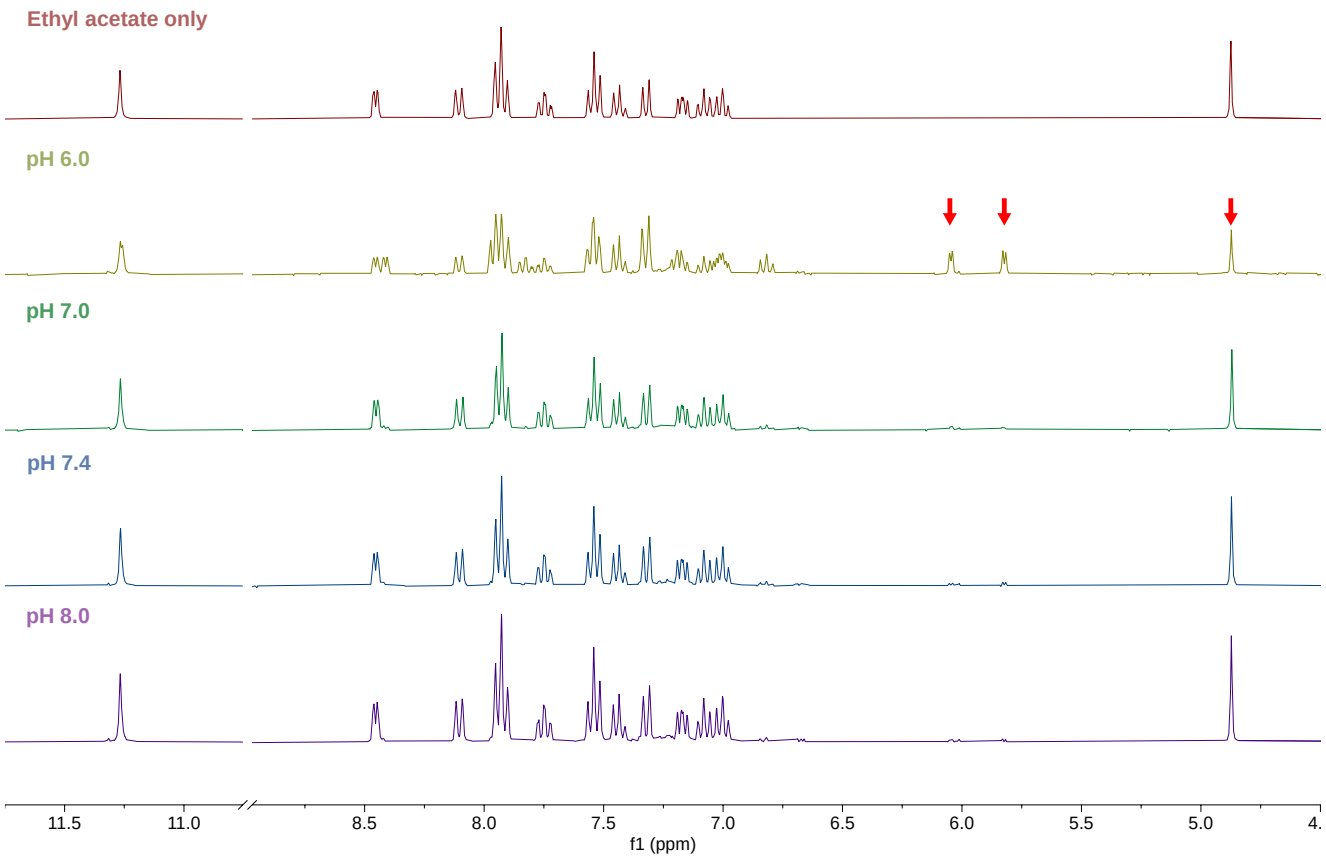


**Figure 7.** $^{1}$H NMR spectra of analogue **13a** after dissolution in phosphate buffers (pH 6-8), extraction with ethyl acetate, and re-dissolution in DMSO-$d_6$. Diagnostic peak changes are indicated with red arrows.

To ensure that PIP-199 was not just a weak competitive inhibitor that could not displace the strong binding MM2-based tracer (SI Figure S13), we subsequently conducted surface plasmon resonance (SPR) assays (20 mM HEPES, 150 mM NaCl, 0.005% Tween, 5%v/v DMSO, pH 7.5) to quantify binding to RMI1/RMI2. While solubility issues were encountered at high concentrations leading to poor surface behavior, we found no convincing evidence of PIP-199 or its analogues (**13a**,**c**-**d**, **14**) binding to RMI1/RMI2 under all experimental conditions tested (SI Figure S14-19).

## CONCLUSIONS

In this study, we have reported the synthesis of PIP-199 and characterized its inherent chemical instability in organic solvents and aqueous buffers. The primary mode of degradation appears to be the loss of the piperazine moiety to form a stable indolic nitrone, which can subsequently be hydrated to form the corresponding alcohol and a mixture of other minor byproducts.

We have also designed more stable analogues by removing the *N*-hydroxy functionality of PIP-199, leading to a series of compounds that are stable in organic solvents and non-acidic aqueous buffers. Nevertheless, the clear propensity for this family of Mannich-derived scaffolds (Figure 1) to degrade in aqueous or mildly acidic media remains a clear liability. When compounds in this family arise in future screens, they should be flagged for stability testing before proceeding any further.

Neither PIP-199 nor its more stable analogues showed any competitive inhibition or binding activity in FP and SPR assays respectively. While we cannot rule out the minor possibility that small details in the way that assay protocols were conducted could have been responsible for the discrepancy between our data and previous published reports, we note that our buffer conditions were chosen to be comparable to those reported in the original screening campaign, and notably, these are conditions under which PIP-199 is conclusively unstable.

Based on the accumulated evidence from our biophysical assays on recombinant RMI1/RMI2, PIP-199 does not appear to be a selective inhibitor for the FANCM-RMI interaction as reported in the literature. We conclude that in the diverse biological experiments where PIP-199 and related structures were used to study ALT, quorum sensing, and other fundamental biological phenomena, any apparent functional activity of PIP-199 is likely a consequence of non-specific off-target effects arising from a mixture of breakdown products. Thus to date, there are still no known chemical inhibitors of the FANCM-RMI interaction in the literature.

Our study reinforces the importance of independently validating compounds derived from library screens, not only for *in vitro* target engagement, but also in terms of chemical stability under common assays conditions. As with other PAINS and IMPs, awareness of potential problems and early prioritization of hit validation experiments can

prevent unproductive research effort being spent on problematic chemical scaffolds and candidate inhibitors, let alone the impact of unreliable biological findings arising from the use of unvalidated inhibitors.

## EXPERIMENTAL SECTION

**General procedures.** All reactions were conducted using dry glassware and under an inert nitrogen atmosphere unless otherwise specified. Chemical reagents were purchased and used without further purification. Anhydrous solvents were obtained from a PureSolv MD7 (Inert Corporation) and used as obtained. Thin-layer chromatography was performed on aluminum-backed silica gel 60 F254, 200 μM plates (ChemSupply). Column chromatography was performed on a Biotage® Selekt using Silica Gel 60 LR 0.04-0.06 mm (230-400 mesh ASTM) (ChemSupply). Nuclear magnetic resonance (NMR) was performed using a Bruker 300 or 500 MHz Spectrometer. NMR were assigned using COSY, HSQC and HMBC where required. Where DMSO-$d_6$ was used as the solvent and internal lock, spectra were referenced to residual solvent for DMSO ($\delta_H$ 2.50 ppm) for $^1$H NMR and ($\delta_C$ 39.5 ppm) for $^{13}$C NMR. For $CDCl_3$, spectra were referenced to residual $CHCl_3$ ($\delta_H$ 7.26 ppm) for $^1$H NMR and ($\delta_C$ 77.0 ppm) for $^{13}$C NMR. Chemical shift values are reported in parts per million, $^1$H-$^1$H coupling constants are reported in hertz and H multiplicity is abbreviated as; s = singlet, d = doublet, t = triplet, q = quartet, m = multiplet, br = broad signal. Infra-red spectra were obtained on a Bruker Alpha-E FT-IR spectrometer fitted with an attenuated total reflectance (ATR) sampling accessory. Absorption maxima are reported in wavenumbers (cm$^{-1}$). Melting point was recorded using OptiMelt MPA100 melting point apparatus (Stanford Research System). High resolution mass spectra was obtained on a Bruker Solarix 2XR magnetic resonance mass spectrometry using either electrospray ionization or atmospheric pressure chemical ionization.

**2-Phenyl-1*H*-indol-1-ol (12).** This method was adapted from previously reported literature.[31] Benzoin oxime (254 mg, 1.12 mmol) was dissolved in concentrated sulfuric acid (5 mL) and the reaction mixture was stirred at room temperature until the reaction mixture turned dark red after approximately 2 h. The crude product was precipitated after quenching on ice and filtered to give a pale-yellow powder. Recrystallization from 2-isopropanol gave the desired product as a yellow crystalline solid (213 mg, 1.02 mmol, 91%). M.p. 128 °C (Decomposed). $^1$H NMR (500 MHz, DMSO-$d_6$) δ 11.16 (s, 1H), 7.89 (d, *J* = 7.3 Hz, 2H), 7.55 (d, *J* = 7.9 Hz, 1H), 7.49 (t, *J* = 7.7 Hz, 2H), 7.44 (d, *J* = 8.2 Hz, 1H), 7.38 (t, *J* = 7.5 Hz, 1H), 7.19 (t, *J* = 7.6 Hz, 1H), 7.05 (t, *J* = 7.5 Hz, 1H), 6.64 (s, 1H); $^{13}$C NMR (126 MHz, DMSO-$d_6$) δ 137.4, 135.9, 131.4, 129.0 (overlapping peaks), 128.2, 123.5, 122.3, 120.7, 120.2, 109.3, 96.6. NMR spectra match those previously reported in the literature.[32]

**General procedure for the Mannich reaction.** To 1 equivalent of corresponding aldehyde (1.00 mmol) was added 1 equivalent of acetic acid and 1.1 equivalents of secondary amine. The mixture was diluted with minimum amount of acetonitrile (~ 1.5 mL) and stirred at room temperature. After 45 min, 1 equivalent of the appropriate aromatic nucleophile was dissolved in minimum amount of acetonitrile (~ 3 mL) and added into the reaction mixture dropwise over 1 min. The reaction was stirred at room temperature for a further 2 h, then purified as follows unless otherwise specified. The reaction mixture was taken up in ethyl acetate (20 mL), washed with water (3 × 20 mL), brine (20 mL), dried over $Na_2SO_4$ and concentrated in *vacuo*. The crude product was purified *via* silica flash chromatography using different solvent mixtures as specified for each compound.

**Ethyl 4-((1-hydroxy-2-phenyl-1*H*-indol-3-yl)(pyridin-2-yl)methyl)piperazine-1-carboxylate (PIP-199, 1).** Picolinaldehyde (76.8 mg, 0.717 mmol), ethyl piperazine-1-carboxylate (125 mg, 0.789 mmol), acetic acid (45.2 mg, 0.753 mmol) and 2-phenyl-1*H*-indol-1-ol (150 mg, 0.717 mmol) were reacted according to the general Mannich procedure. The reaction mixture was cooled to 0 °C to precipitate the product. Filtration and washing with cold dry acetonitrile yielded the product as a white amorphous solid (157 mg, 0.344 mmol, 48%). $^1$H NMR (500 MHz, DMSO-$d_6$) δ 10.86 (s, 1H), 8.43 (d, *J* = 3.0 Hz, 1H), 8.05 (d, *J* = 8.1 Hz, 1H), 7.84 (d, *J* = 8.0 Hz, 1H), 7.80 (d, *J* = 7.1 Hz, 2H), 7.74 (td, *J* = 7.7, 1.9 Hz, 1H), 7.55 (t, *J* = 7.6 Hz, 2H), 7.51 – 7.44 (m, 1H), 7.36 (d, *J* = 8.2 Hz, 1H), 7.13 – 7.20 (m, 2H), 7.04 (t, *J* = 7.6 Hz, 1H), 4.70 (s, 1H), 3.99 (q, *J* = 7.1 Hz, 2H), 2.34 – 2.17 (m, 4H), 1.13 (t, *J* = 7.1 Hz, 3H); $^{13}$C NMR (126 MHz, DMSO-$d_6$) δ 161.9, 154.5, 148.8, 136.6, 136.5, 134.5, 131.0, 129.7, 128.09, 128.06, 121.9, 121.8, 121.6, 121.1, 120.9, 119.6, 108.8, 107.4, 69.1, 60.7, 51.3, 43.6, 14.6.; IR (ATR) 2507 cm$^{-1}$, 1698 cm$^{-1}$, 1433 cm$^{-1}$, 1242 cm$^{-1}$, 1001 cm$^{-1}$, 737 cm$^{-1}$; HRMS (ESI) calcd for $C_{27}H_{29}N_4O_3$ $[M + H]^+$ 457.2234, found 457.2231 (error -0.721748 ppm).

**Ethyl 4-((2-phenyl-1*H*-indol-3-yl)(pyridin-2-yl)methyl)piperazine-1-carboxylate (13a).** Picolinaldehyde (107 mg, 1.00 mmol), ethyl piperazine-1-carboxylate (174 mg, 1.10 mmol), acetic acid (60.1 mg, 1.00 mmol) and 2-phenyl-1*H*-indole (193 mg, 1.00 mmol) were reacted according to the general Mannich procedure. The crude product was purified by flash chromatography using a gradient of 15-35% ethyl acetate in hexane over 15 column volumes, with the product eluting at 35% ethyl acetate, yielding an amorphous white solid (192 mg, 0.436 mmol, 44 %). $^1$H NMR (500 MHz, DMSO-$d_6$) δ 11.28 (s, 1H), 8.46 (d, *J* = 4.2 Hz, 1H), 8.11 (d, *J* = 8.0 Hz, 1H), 7.95 (d, *J* = 7.0 Hz, 2H), 7.92 (d, *J* = 7.8 Hz, 1H), 7.75 (td, *J* = 7.7, 1.9 Hz, 1H), 7.55 (t, *J* = 7.6 Hz, 2H), 7.44 (t, *J* = 7.4 Hz, 1H), 7.33 (d, *J* = 8.0 Hz, 1H), 7.18 (dd, *J* = 7.4, 4.9 Hz, 1H), 7.09 (t, *J* = 7.6 Hz, 1H), 7.01 (t, *J* = 7.6 Hz, 1H), 4.88 (s, 1H), 3.99 (q, *J* = 7.1 Hz, 2H), 2.34 – 2.19 (m, 4H), 1.13 (t, *J* = 7.1 Hz, 3H); $^{13}$C NMR (126 MHz, DMSO-$d_6$) δ 162.8, 155.0, 149.2, 137.2, 137.1, 136.7, 133.1, 129.8, 128.9, 128.3, 126.8, 122.3, 122.1, 122.0, 121.4, 119.6, 111.8, 111.1, 69.5, 61.1, 51.8, 44.1, 15.0; IR (ATR) 3309, 1664, 1432, 1247, 772, 740, 699 cm$^{-1}$; HRMS (ESI) calcd for $C_{27}H_{28}N_4NaO_2$ $[M + H]^+$ 463.2105, found 463.2100 (error -0.885127 ppm).

**Ethyl 4-(phenyl(2-phenyl-1H-indol-3-yl)methyl)piperazine-1-carboxylate (13b).** Benzaldehyde (27.7 mg, 0.259 mmol), ethyl piperazine-1-carboxylate (45.0 mg, 0.285 mmol), acetic acid (15.5 mg, 0.259 mmol) and 2-phenyl-1*H*-indole (50.0 mg, 0.259 mmol) were reacted according to the general Mannich procedure. The crude product was purified *via* the same procedure as **13a**, yielding an amorphous white solid (55.0 mg, 0.125 mmol, 48%). $^1$H

NMR (500 MHz, DMSO-$d_6$) δ 11.23 (s, 1H), 8.10 (d, *J* = 8.0 Hz, 1H), 7.58 – 7.52 (m, 4H), 7.46 (t, *J* = 6.7 Hz, 1H), 7.35 – 7.29 (m, 3H), 7.20 (t, *J* = 7.5 Hz, 2H), 7.09 (q, *J* = 7.8 Hz, 2H), 7.01 (t, *J* = 7.5 Hz, 1H), 4.73 (s, 1H), 4.00 (q, *J* = 7.1 Hz, 2H), 3.38 (s, 4H), 2.42 – 2.28 (m, 4H), 1.14 (t, *J* = 7.0 Hz, 3H); $^{13}$C NMR (126 MHz, DMSO-$d_6$) δ 155.0, 143.6, 136.6, 133.3, 129.7, 129.1, 128.7, 128.4, 127.8, 126.9, 126.8, 121.9, 121.6, 119.6, 112.6, 111.7, 68.0, 61.1, 51.9, 44.1, 15.1; IR (ATR) 3287, 2923, 1678, 1448, 1247, 1025, 907, 729, 697 cm$^{-1}$; HRMS (ESI) calcd for $C_{28}H_{28}N_3O_2$ $[M + H]^+$ 438.2176, found 438.2173 (error -0.684591 ppm).

**2-Phenyl-3-(piperidin-1-yl(pyridin-2-yl)methyl)-1*H*-indole (13c).** Picolinaldehyde (33.3 mg, 0.310 mmol), piperidine (27.8 mg, 0.326 mmol), acetic acid (18.6 mg, 0.310 mmol) and 2-phenyl-1*H*-indole (60.0 mg, 0.310 mmol) were reacted according to the general Mannich procedure. The crude product was purified using flash chromatography using a gradient of 1-5% methanol in dichloromethane over 15 column volumes, with the product eluting at 3% methanol, yielding an amorphous white solid (38.4 mg, 0.103 mmol, 33%). $^1$H NMR (400 MHz, DMSO-$d_6$) δ 11.19 (s, 1H), 8.43 (ddd, *J* = 4.8, 1.9, 0.9 Hz, 1H), 8.11 (d, *J* = 7.9 Hz, 1H), 8.02 – 7.93 (m, 2H), 7.92 (dt, *J* = 8.0, 1.1 Hz, 1H), 7.73 (td, *J* = 7.7, 1.9 Hz, 1H), 7.54 (dd, *J* = 8.3, 7.0 Hz, 2H), 7.47 – 7.38 (m, 1H), 7.31 (dt, *J* = 8.0, 1.0 Hz, 1H), 7.14 (ddd, *J* = 7.4, 4.9, 1.2 Hz, 1H), 7.07 (ddd, *J* = 8.1, 7.0, 1.3 Hz, 1H), 6.99 (ddd, *J* = 8.0, 7.0, 1.2 Hz, 1H), 4.84 (s, 1H), 2.35 – 2.14 (m, 4H), 1.52 – 1.42 (m, 4H), 1.41 – 1.32 (m, 2H); $^{13}$C NMR (101 MHz, DMSO-$d_6$) δ 163.5, 148.7, 136.6, 136.6, 136.4, 133.0, 129.5, 128.6, 127.8, 126.7, 121.72, 121.69, 121.5, 121.3, 119.1, 111.7, 111.4, 69.9, 52.9, 40.4, 40.2, 39.9, 39.7, 39.5, 39.3, 39.1, 26.1, 24.5; IR (ATR) 3189, 2912, 2785, 2746, 1587, 1451, 1430, 763, 750, 738, 697, 570 cm$^{-1}$; HRMS (APCI) calcd for $C_{25}H_{26}N_3$ $[M + H]^+$ 368.2121, found 368.2130 (error 2.444243 ppm).

**Ethyl 4-((2-methyl-1*H*-indol-3-yl)(pyridin-2-yl)methyl)piperazine-1-carboxylate (13d).** Picolinaldehyde (118 mg, 1.10 mmol), ethyl piperazine-1-carboxylate (191 mg, 1.21 mmol), acetic acid (66.1 mg, 1.10 mmol) and 2-methyl-1*H*-indole (144 mg, 1.10 mmol) were reacted according to the general Mannich procedure. The crude product was purified *via* the same procedure as **13a**, yielding an amorphous orange solid (112 mg, 0.296 mmol, 27%). $^1$H NMR (500 MHz, DMSO) δ 10.81 (s, 1H), 8.38 (d, *J* = 4.3 Hz, 1H), 7.86 (d, *J* = 7.6 Hz, 1H), 7.74 (d, *J* = 7.9 Hz, 1H), 7.69 (td, *J* = 7.6, 1.8 Hz, 1H), 7.18 (d, *J* = 7.8 Hz, 1H), 7.13 (ddd, *J* = 6.7, 4.8, 1.3 Hz, 1H), 6.99 – 6.88 (m, 2H), 4.67 (s, 1H), 4.01 (q, *J* = 7.0 Hz, 2H), 3.40 (s, 4H), 2.44 (s, 3H), 2.42 – 2.25 (m, 4H), 1.15 (t, *J* = 7.1 Hz, 3H); $^{13}$C NMR (126 MHz, DMSO) δ 163.1, 155.1, 149.1, 137.0, 135.7, 133.7, 126.9, 122.2, 121.5, 120.5, 119.7, 119.1, 110.9, 110.0, 70.3, 61.1, 51.8, 44.1, 15.1, 12.5; IR (ATR) 3179, 2975, 2811, 2754, 1692,1424, 1237, 1124, 994, 764, 740 cm$^{-1}$; HRMS (ESI) calcd for $C_{22}H_{26}N_4NaO_2$ $[M + Na]^+$ 401.1948, found 401.1945 (error -0.747766ppm).

**Ethyl 4-((1-hydroxynaphthalen-2-yl)(pyridin-2-yl)methyl)piperazine-1-carboxylate (14).** Picolinaldehyde (37.2 mg, 0.347 mmol), ethyl piperazine-1-carboxylate (57.6 mg, 0.364 mmol), acetic acid (20.8 mg, 0.347 mmol) and naphthalen-1-ol (50.0 mg, 0.347 mmol) were reacted according to the general Mannich procedure. The crude product was purified *via* the same procedure as **13a**, yielding an amorphous yellow solid (67.0 mg, 0.171 mmol, 49%). $^1$H NMR (400 MHz, DMSO) δ 11.72 (s, 1H), 8.55 (dd, *J* = 5.0, 1.8 Hz, 1H), 8.20 – 8.11 (m, 1H), 7.83 – 7.72 (m, 2H), 7.59 (d, *J* = 7.9 Hz, 1H), 7.47 – 7.41 (m, 2H), 7.31 – 7.23 (m, 3H), 4.82 (s, 1H), 4.02 (q, *J* = 7.1 Hz, 2H), 3.43 (t, *J* = 5.4 Hz, 4H), 2.48 – 2.30 (m, 4H), 1.15 (t, *J* = 7.0 Hz, 3H). $^{13}$C NMR (101 MHz, DMSO) δ 159.6, 154.5, 151.4, 149.3, 137.6, 133.5, 127.5, 127.2, 126.2, 124.9, 124.8, 123.2, 123.0, 122.1, 118.5, 117.6, 75.0, 60.8, 50.8, 43.3, 40.2, 40.1, 39.9, 39.7, 39.5, 39.3, 39.1, 38.9, 14.6; IR (ATR) 2810, 1690, 1431, 1384, 1289, 1246, 1224, 1120, 1084, 993, 799, 746, 685 cm$^{-1}$; HRMS (APCI) calcd for $C_{23}H_{25}N_3O$ $[M + H]^+$ 391.1890, found 391.1900 (error 2.377367 ppm).

**Partial purification of decomposition product 2-Phenyl-3-(pyridin-2-ylmethylene)-3H-indole 1-oxide (15).** PIP-199 (10 mg) was dissolved in $CDCl_3$ (10 mL) and mixed until fully dissolved which typically indicated full decomposition. The resulting mixed was washed with water (4 × 10 mL), brine (10 mL), dried with $Na_2SO_4$ then concentrated *in vacuo* to yield a dark red solid (5 mg). The product could not fully be purified due to additional decomposition products forming. $^1$H NMR (300 MHz, DMSO-$d_6$) δ 9.07 (d, *J* = 7.0 Hz, 1H), 8.91 (d, *J* = 3.6 Hz, 1H), 7.93 (td, *J* = 7.7, 1.9 Hz, 1H), 7.88 – 7.78 (m, 2H), 7.77 (d, *J* = 8.2 Hz, 2H), 7.72 – 7.53 (m, 5H), 7.54 – 7.43 (m, 1H), 7.30 (s, 1H); IR (ATR) 3053, 2926, 2855, 1698, 1587, 1433, 1239, 1000, 737, 697 cm$^{-1}$; HRMS (ESI) calcd for $C_{20}H_{15}N_2O$, $[M + H]^+$ 299.1179, found 299.1177 (error -0.668633 ppm).

**Aqueous stability studies.** Compounds were dissolved as stock solutions in DMSO at 5 mM concentration. From these stocks, 1 mL was diluted to a final concentration of 250 μM using buffer containing DMSO to aid solubility (16.7%v/v DMSO for phosphate buffers and 50 mM $NH_4Cl$ buffer, 7.5%v/v DMSO for all other buffer conditions). The buffer-diluted solutions were left for 1.5 h and then extracted with ethyl acetate (2 × 5 mL). The extracts were washed with brine (10 mL), dried over $Na_2SO_4$ and concentrated *in vacuo*. The resulting solid residue was re-dissolved in DMSO-$d_6$ for $^1$H NMR analysis (SI Figure S25-26, 28-39).

The negative control involved diluting the DMSO stocks (1 mL of 5 mM stock) directly into ethyl acetate (10 mL) and leaving for 1.5 h. The mixture was washed with brine (10 mL), dried over $Na_2SO_4$ and concentrated *in vacuo*. The resulting solid residue was re-dissolved in DMSO-$d_6$ for $^1$H NMR analysis (SI Figure S24).

In all cases, the pH of the buffers was checked before and after dilution to verify that the pH was maintained. For data processing, the relative proportions of PIP-199, nitrone **15** and alcohol **16** were calculated by normalising the integration values relative to the total integration across all three peaks at δ 4.7 (PIP-199), 5.8 (alcohol **16**) and 7.3 ppm (nitrone **15**) using MestreNova.

**UV-Vis spectroscopy.** All UV-Vis spectroscopy was performed on a Cary 60 UV-Vis spectrometer (Agilent Technologies). Scans were run in scan mode with scanning wavelengths of 200-800 nm and absorbance measured with a scan rate of 600 nm/min in dual beam mode with baseline correction. PIP-199 and crude nitrone **15** were dissolved in DMSO at a final concentration of 50 μM. For attempted kinetic analysis, a 10 mM DMSO stock was diluted in 50 mM potassium phosphate buffer at pH 7 or 8 to a final

concentration of 50 μM, and absorbance at 370 nm (characteristic λ of **15**) was measured every 0.1 sec for a total of 3 min using kinetic mode.

**Liquid chromatography mass spectrometry.** Liquid chromatography mass spectrometry were performed using a Shimadzu Nexera-I LC-2040C Plus coupled to a Shimadzu LCMS-2020 mass spectrometer ESI single quadrupole mass detector (Shimadzu Corporation). Separation was performed by reversed-phase chromatography with a Shimadzu Shim-Pack Sceptor C18-120 (2.1 mm × 100 mm, 3 μM) run at 0.4 mL/min. The mobile phases were run with water (solvent A) and acetonitrile (solvent B) with both containing 0.1 % formic acid. The gradient was programmed as 5-95% B over 12 min. All *m/z* values of eluting ions were measured with an ESI ion source in positive and negative ion mode and scanned between *m/z* 100-1000. Compounds were directly dissolved from solids in a 50:50 mix of $H_2O$:MeCN (<1 mg/mL, typically not fully soluble), filtered (PTFE syringe filter, 0.4 μM) and ran directly on LCMS.

**Recombinant production of RMI1/RMI2.** Commercial bioreagents were used as supplied without further purification. Lysogeny broth (LB) was purchased as pre-mixed powders from Amyl Media and prepared according to the manufacturer's protocol. Lysozyme from chicken egg white, deoxyribonuclease I (DNase) from bovine pancreas, and protease inhibitor cocktail (AEBSF, bestatin, E-64, pepstatin A, phosphoramidon) were purchased from Sigma-Aldrich. Antibiotics were purchased from Pure Science. Ampicillin and carbenicillin were used at 100 μg/mL, with carbenicillin being used in lieu of ampicillin for liquid cultures. SDS-PAGE was performed using Mini-PROTEAN TGX Stain-Free gels (Bio-Rad) with Tris-glycine SDS running buffer. Unstained Protein Standard, Broad Range 10-200 kDa (New England Biolabs) was used as a ladder for all gels.

RMI1/RMI2 production was adapted from previous methods.[15, 33] Two separate RMI proteins were expressed, RMI1/RMI2 and biotinylated RMI1/RMI2 (for immobilization). The sequences for both RMI1/RMI2 proteins were generated by PCR from a construct kindly provided by Assoc. Prof. Andrew Deans using primers (SI Table S1) and subcloned into a pETDuet-1 backbone bearing a *N*-terminal hexahistidine tag and SUMO for RMI1/RMI2, and a *N*-terminal hexahistidine tag and AviTag as well as BirA for biotinylated RMI1/RMI2. Subcloning was done by Gibson assembly using NEBuilder HiFi DNA Assembly Master Mix (New England Biolabs) (SI Table S2). Chemically competent *E. coli* strain DH5α was used for all cloning procedures. Sequences of plasmids were confirmed by Sanger sequencing conducted through the Ramaciotti Centre for Genomics (University of New South Wales, Australia).

The pETDuet plasmids were transformed into BL21(*DE3*) *E. coli* cells. Overnight 5 ml cultures were diluted into 500 ml of fresh LB medium and grown at 37 °C until $OD_{600}$ of 0.4 was achieved. Expression was induced with IPTG (0.1 mM), and the cells were incubated at 18 °C overnight. For biotinylated AviTag RMI1/RMI2, biotin (50 μM) was added during induction. Cells were then pelleted by centrifugation at 3900 relative centrifugal force (rcf) for 15 min and stored at −20 °C.

Frozen cell pellets were resuspended in 20 ml of lysis buffer (50 mM Tris, 400 mM NaCl, 10% glycerol, pH 8) followed by addition of 2-mercaptoethanol (2 mM), DNAse (100 μg/ml), lysozyme (100 μg/ml) and protease inhibitor cocktail (400 μL, Roche) and incubated on ice for 10 min before sonicating (45% amps, 8 sec on, 10 sec off for 20 min) on ice (Sonopuls HD 4050 probe sonicator with a TS-106 probe, Bandelin). The lysate was clarified by centrifugation (7197 rcf for 20 min). The supernatant containing protein was collected and incubated with HisPur Ni-NTA resin (2 mL, Thermo Fisher Scientific) by stirring on ice for 1 h. The resin with bound protein was poured into a column and washed with buffer (50 mM Tris, 400 mM NaCl, 10% glycerol, 20 mM imidazole, 2 × 20 mL) then RMI1/RMI2 was eluted in buffer (50 mM Tris, 400 mM NaCl, 10% glycerol, 500 mM imidazole, 30 mL). Collected fractions were analysed by SDS-PAGE (SI Figure S20 and S22) and fractions containing the desired protein were pooled and concentrated (3 kDa MWCO, Amicon) then buffer exchanged (50 mM Tris, 400 mM NaCl, 10% glycerol, 2 mM 2-mercaptoethanol) until concentration of imidazole was <20 mM. Biotinylated RMI was carried directly to SEC purification.

For cleavage of the His-SUMO tag from RMI1/RMI2, hexahistidine-tagged SenP2 protease (1:250 equivalents from a 10 μM stock) was added to the affinity purified protein and left overnight at room temperature. The resulting solution was again purified by incubating with Ni-NTA resin (2 mL) on ice for 1 h before collecting the flow through containing cleaved RMI1/RMI2. Collected fractions were pooled and concentrated (3kDa MWCO, Amicon) and stored at 4 °C until purification by SEC. For AviTag proteins, the affinity tag was not removed.

Proteins were purified by FPLC using an Akta Pure M2 equipped with HiLoad 16/600 Superdex 200 pg column at a flow rate of 0.5 ml/min in buffer (50 mM Tris, 200 mM NaCl, 10% glycerol, 2 mM 2-mercaptoethanol). Fractions containing protein were identified by SDS-PAGE (SI Figure S20-23), pooled, and concentrated (3 kDa MWCO, Amicon). Protein concentration was checked by absorbance at 280 nm, aliquoted, then flash frozen and stored at –80 °C until use.

**Competitive fluorescence polarization assay.** The fluorescent tracer probe used was a 20-mer derived from the MM2 domain of FANCM with the sequence (5-TAMRA)-SRDLFSVTFDLGFCSPDSDD-$NH_2$ (Mimotopes). Direct titration of RMI1/RMI2 against this TMR-MM2 tracer showed the expected binding with an $IC_{50}$ 21 ± 8 nM (SI Figure S9). The affinity of TMR-MM2 was independently determined by SPR to be 0.3 ± 0.004 nM (SI Figure S13).

The protein target RMI1/RMI2 (100 nM) and TMR-MM2 (20 nM) were mixed in assay buffer A (50 mM Tris pH 8, 200 mM NaCl, 2 mM 2-mercaptoethanol) or assay buffer B (10 mM Tris pH 8.8, 40 mM NaCl, 2 mM 2-mercaptoethanol) and 20 μL per well was dispensed into black 384-well plates with a non-binding surface (Corning 3820). Compounds were diluted in assay buffer from DMSO stocks (7.5 %v/v DMSO) and two-fold serial dilutions performed to obtain 16 titration data points, then 20 μL of each dilution was added to the appropriate wells (final conditions 3.75 %v/v DMSO, RMI1/RMI2 = 25 nM, TMR-MM2 = 5 nM) and left to incubate for 1 h at room temperature in the dark.

Anisotropy was measured on a BMG Labtech PHERAstar FSX Multimodal Plate Reader with a TAMRA Fluorescence Polarisation Optic Module 540/590/590. Data was

processed by normalising to the positive (tracer only) and negative (tracer and protein only) controls and represented as percentage of tracer bound and graphed using GraphPad Prism 9.4.1 non-linear regression.

**Surface plasmon resonance assay.** SPR was performed on a Biacore T200 instrument (GE healthcare) using a CM5 senor chip (GE healthcare). Running buffer was 20 mM HEPES, 150 mM NaCl, 0.005% Tween, 5% DMSO pH 7.5, and all analysis was carried out at 15 $^{0}$C. Biotinylated Avi-tagged RMI1/RMI2 heterodimer was immobilized on the chip using standard affinity capture to streptavidin up to a density of 10000 response units (RU). Small molecules were assayed using multiple cycle kinetics over a concentration range of 12.5 – 200 μM. A variant of the native MM2 peptide was used as the positive control over a concentration range of 0.01 – 15 μM to give saturable binding (SI Figure S14). For all experiments contact time was 60 s, dissociation time was 60 s, with a flow-rate of 40 μL/min. All data were reference subtracted. Kinetic constants were determined by fitting the data using affinity screen with a 1:1 binding model (Biacore T200 Evaluation Software).

### ASSOCIATED CONTENT

**Supporting Information**. Additional experimental results including NMR of stability studies, LCMS of decomposition products, UV-Vis data, FP assay data, SPR assay data, protein production, and full characterization of all compounds.

## AUTHOR INFORMATION


### Corresponding Authors

*Email addresses: yuheng.lau@sydney.edu.au; lisa.alcock@sydney.edu.au


### Author Contributions

The manuscript was written through contributions of all authors. All authors have given approval to the final version of the manuscript.


### Funding Sources

YHL acknowledges funding from the National Health and Medical Research Council (Ideas Grant 2003250, MRFF Grant 2007488). LJA acknowledges funding from the Tour de Cure Foundation (RSP-329-FY2023).


## ACKNOWLEDGMENTS


We thank Sydney Analytical for providing access and staff support for NMR and SPR instrumentation, and Assoc. Prof. Andrew Deans (St Vincent's Institute of Medical Research, Melbourne) for providing plasmids containing the RMI1/RMI2 gene sequences. We also thank Prof. Hilda Pickett for sharing her insight into ALT cell biology and expertise in studying the FANCM-RMI interaction.


## ABBREVIATIONS

ALT, alternative lengthening of telomeres; APCI, atmospheric pressure chemical ionization; FANCM, Fanconi Anemia complementation group M; FP, fluorescence polarization; HRMS, high resolution mass spectrometry; IMPs, invalid metabolic panaceas; LCMS, liquid chromatography mass spectrometry; PAINS, pan-assay interference compounds; RMI, RecQ mediated genome instability protein; SPR, surface plasmon resonance; TLC, thin layer chromatography.

## REFERENCES


1. Arrowsmith, C. H.; Audia, J. E.; Austin, C.; Baell, J.; Bennett, J.; Blagg, J.; Bountra, C.; Brennan, P. E.; Brown, P. J.; Bunnage, M. E.; Buser-Doepner, C.; Campbell, R. M.; Carter, A. J.; Cohen, P.; Copeland, R. A.; Cravatt, B.; Dahlin, J. L.; Dhanak, D.; Edwards, A. M.; Frederiksen, M.; Frye, S. V.; Gray, N.; Grimshaw, C. E.; Hepworth, D.; Howe, T.; Huber, K. V. M.; Jin, J.; Knapp, S.; Kotz, J. D.; Kruger, R. G.; Lowe, D.; Mader, M. M.; Marsden, B.; Mueller-Fahrnow, A.; Müller, S.; O'Hagan, R. C.; Overington, J. P.; Owen, D. R.; Rosenberg, S. H.; Ross, R.; Roth, B.; Schapira, M.; Schreiber, S. L.; Shoichet, B.; Sundström, M.; Superti-Furga, G.; Taunton, J.; Toledo-Sherman, L.; Walpole, C.; Walters, M. A.; Willson, T. M.; Workman, P.; Young, R. N.; Zuercher, W. J., The promise and peril of chemical probes. *Nat. Chem. Bio.* **2015,** *11* (8), 536-541.
2. Baell, J.; Walters, M. A., Chemistry: Chemical con artists foil drug discovery. *Nature* **2014,** *513* (7519), 481-483.
3. Bisson, J.; McAlpine, J. B.; Friesen, J. B.; Chen, S.-N.; Graham, J.; Pauli, G. F., Can invalid bioactives undermine natural product-based drug discovery? *J. Med. Chem.* **2016,** *59* (5), 1671-1690.
4. Nelson, K. M.; Dahlin, J. L.; Bisson, J.; Graham, J.; Pauli, G. F.; Walters, M. A., The essential medicinal chemistry of curcumin. *J. Med. Chem.* **2017,** *60* (5), 1620-1637.
5. Baell, J. B.; Nissink, J. W. M., Seven year itch: Pan-Assay Interference Compounds (PAINS) in 2017—utility and limitations. *ACS Chem. Bio.* **2018,** *13* (1), 36-44.
6. Padmanaban, G.; Nagaraj, V. A., Curcumin may defy medicinal chemists. *ACS Med. Chem. Lett.* **2017,** *8* (3), 274-274.
7. Baell, J. B.; Holloway, G. A., New substructure filters for removal of Pan Assay Interference Compounds (PAINS) from screening libraries and for their exclusion in bioassays. *J. Med. Chem.* **2010,** *53* (7), 2719-2740.
8. Voter, A. F.; Manthei, K. A.; Keck, J. L., A high-throughput screening strategy to identify protein-protein interaction inhibitors that block the fanconi anemia DNA repair pathway. *J. Biomol. Screen.* **2016,** *21* (6), 626-633.
9. Deans, A. J.; West, S. C., FANCM connects the genome instability disorders Bloom's Syndrome and Fanconi anemia. *Mol. Cell* **2009,** *36* (6), 943-953.
10. Lu, R.; O'Rourke, J. J.; Sobinoff, A. P.; Allen, J. A. M.; Nelson, C. B.; Tomlinson, C. G.; Lee, M.; Reddel, R. R.; Deans, A. J.; Pickett, H. A., The FANCM-BLM-TOP3A-RMI complex suppresses alternative lengthening of telomeres (ALT). *Nat. Comm.* **2019,** *10* (1), 2252.
11. Yang, S. Y.; Chang, E. Y. C.; Lim, J.; Kwan, H. H.; Monchaud, D.; Yip, S.; Stirling, Peter C.; Wong, J. M. Y., G-quadruplexes mark alternative lengthening of telomeres. *NAR Cancer* **2021,** *3* (3).
12. O'Rourke, J. J.; Bythell-Douglas, R.; Dunn, E. A.; Deans, A. J., ALT control, delete: FANCM as an anti-cancer target in Alternative Lengthening of Telomeres. *Nucleus* **2019,** *10* (1), 221-230.
13. Baillie, K. E.; Stirling, P. C., Beyond Kinases: Targeting Replication Stress Proteins in Cancer Therapy. *Trends in Cancer* **2021,** *7* (5), 430-446.
14. Gao, J.; Pickett, H. A., Targeting telomeres: advances in telomere maintenance mechanism-specific cancer therapies. *Nat. Rev. Cancer* **2022,** *22* (9), 515-532.

15. Hoadley, K. A.; Xu, D.; Xue, Y.; Satyshur, K. A.; Wang, W.; Keck, J. L., Structure and cellular roles of the RMI core complex from the Bloom syndrome dissolvasome. *Structure* **2010,** *18* (9), 1149-1158.
16. Yu, Q.; Gates, P. B.; Rogers, S.; Mikicic, I.; Elewa, A.; Salomon, F.; Lachnit, M.; Caldarelli, A.; Flores-Rodriguez, N.; Cesare, A. J.; Simon, A.; Yun, M. H., Telomerase-independent maintenance of telomere length in a vertebrate. *bioRxiv* **2022**, 2022.03.25.485759.
17. Christensen, Q. H.; Grove, T. L.; Booker, S. J.; Greenberg, E. P., A high-throughput screen for quorum-sensing inhibitors that target acyl-homoserine lactone synthases. *Proc. Natl. Acad. Sci. USA* **2013,** *110* (34), 13815-13820.
18. Brahmbhatt, H.; Uehling, D.; Al-awar, R.; Leber, B.; Andrews, D., Small molecules reveal an alternative mechanism of Bax activation. *Biochem. J.* **2016,** *473* (8), 1073-1083.
19. Lyu, H.; Petukhov, P. A.; Banta, P. R.; Jadhav, A.; Lea, W. A.; Cheng, Q.; Arnér, E. S. J.; Simeonov, A.; Thatcher, G. R. J.; Angelucci, F.; Williams, D. L., Characterization of lead compounds targeting the selenoprotein thioredoxin glutathione reductase for treatment of schistosomiasis. *ACS Infect. Dis.* **2020,** *6* (3), 393-405.
20. Zorn, K. M.; Sun, S.; McConnon, C. L.; Ma, K.; Chen, E. K.; Foil, D. H.; Lane, T. R.; Liu, L. J.; El-Sakkary, N.; Skinner, D. E.; Ekins, S.; Caffrey, C. R., A machine learning strategy for drug discovery identifies anti-schistosomal small molecules. *ACS Infect. Dis.* **2021,** *7* (2), 406-420.
21. Nolan, T. L.; Geffert, L. M.; Kolber, B. J.; Madura, J. D.; Surratt, C. K., Discovery of novel-scaffold monoamine transporter ligands via in silico screening with the S1 pocket of the serotonin transporter. *ACS Chem. Neurosci.* **2014,** *5* (9), 784-792.
22. Gerdt, J. P.; Blackwell, H. E., Competition studies confirm two major barriers that can preclude the spread of resistance to quorum-sensing inhibitors in bacteria. *ACS Chem. Bio.* **2014,** *9* (10), 2291-2299.
23. Kundu, D.; Bagdi, A. K.; Majee, A.; Hajra, A., Zwitterionic-type molten salt: A mild and efficient organocatalyst for the synthesis of 3-aminoalkylated indoles via three-component coupling reaction. *Synlett* **2011,** *2011* (08), 1165-1167.
24. Pape, V. F. S.; Palkó, R.; Tóth, S.; Szabó, M. J.; Sessler, J.; Dormán, G.; Enyedy, É. A.; Soós, T.; Szatmári, I.; Szakács, G., Structure–activity relationships of 8-hydroxyquinoline-derived mannich bases with tertiary amines targeting multidrug-resistant cancer. *J. Med. Chem.* **2022,** *65* (11), 7729-7745.
25. Ansorge, S., Bank, U., Nordhoff, K., Tager, M., Striggow, F. Dual alanyl aminopeptidase and dipeptidyl peptidase IV inhibitors for functionally influencing different cells and for treating immunological, inflammatory, neuronal and other diseases. Patent WO2005034940. April 21st, 2005.
26. Walensky, L. D., Stewart, M. L., Cohen, N. Small molecules for the modulation of MCL-1 and methods of modulating cell death, cell division, cell differentiation and methods of treating hyperproliferative and other disorders. Patent WO2011094708A2. August 4th, 2011.
27. Trent, J. O., Meier, J. B, Napier, K. B. Compounds for treating disease, for administering, and for pharmaceutical compositions. Patent WO2011127333A2. October 13th, 2011.
28. Pickett, H. A., Azzalin, C. M., Sobinoff, A. P. Treatment of Alternative Lengthening of Telomeres (ALT) cancers based on inhibiting FANCM activity or expression using a genetic inhibitor, small molecule, peptide, or protein. Patent WO2020242330A2. December 3rd, 2020.
29. Mousseron-Canet, M.; Boca, J. P.; Tabacik, V., Tautomérisation du méthyl-2-indolénine N-oxyde en solution. *Spectrochim. Acta A Mol. Spectrosc.* **1967,** *23* (3), 717-725.
30.Hoadley, K. A.; Xue, Y.; Ling, C.; Takata, M.; Wang, W.; Keck, J. L., Defining the molecular interface that connects the Fanconi anemia protein FANCM to the Bloom syndrome dissolvasome. *PNAS* **2012,** *109* (12), 4437-4442.
31. Hill, J. H. M.; Gilbert, D. P.; Feldsott, A. H., Benzoin oximes in sulfuric acid. Cyclization and fragmentation. *J. Org. Chem.* **1975,** *40* (25), 3735-3740.
32. Zhao, Y.; Zhu, H.; Sung, S.; Wink, D. J.; Zadrozny, J. M.; Driver, T. G., Counterion control of t-BuO-mediated single electron transfer to nitrostilbenes to construct N-hydroxyindoles or oxindoles. *Angew. Chem. Int. Ed.* **2021,** *60* (35), 19207-19213.
33. Xu, D.; Guo, R.; Sobeck, A.; Bachrati, C. Z.; Yang, J.; Enomoto, T.; Brown, G. W.; Hoatlin, M. E.; Hickson, I. D.; Wang, W., RMI, a new OB-fold complex essential for Bloom syndrome protein to maintain genome stability. *Genes Dev.* **2008,** *22* (20), 2843-2855.

TOC graphic

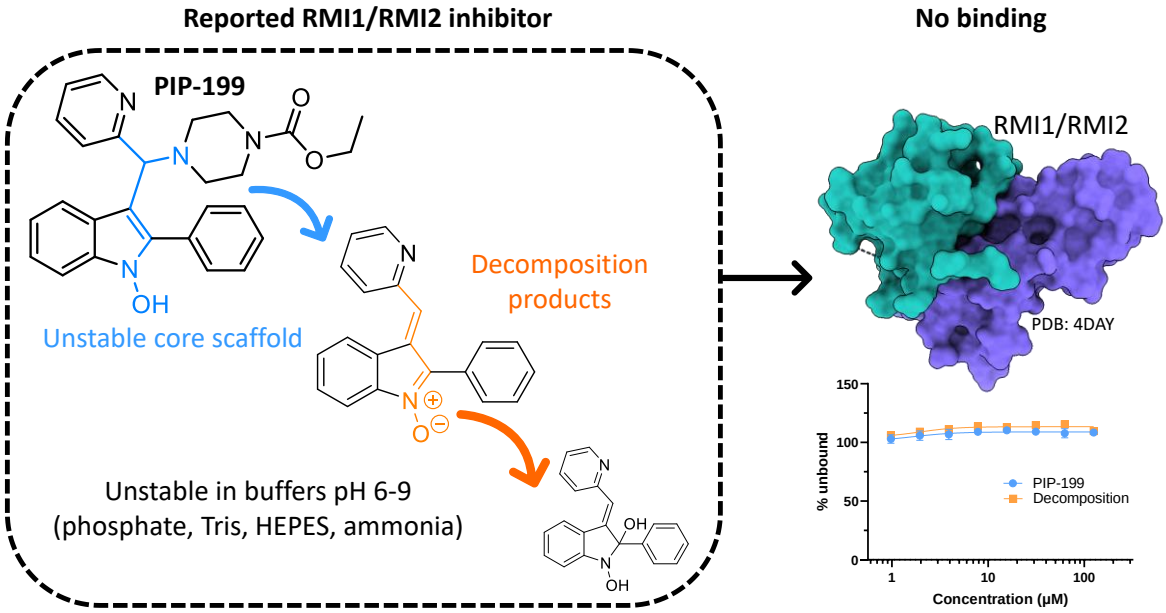
Reported RMI1/RMI2 inhibitor
No binding
PIP-199
Unstable core scaffold
Decomposition products
Unstable in buffers pH 6-9
(phosphate, Tris, HEPES, ammonia)
RMI1/RMI2
PDB: 4DAY
% unbound
PIP-199
Decomposition
Concentration (μM)